



## Small-angle neutron scattering study of shear-induced phase separation in aqueous poly(*N*-isopropylacrylamide) solutions

Markus Stieger<sup>1</sup>, Peter Lindner<sup>2</sup>, Walter Richtering<sup>3</sup>\*

<sup>1</sup> Institute of Physical Chemistry, University of Kiel, Olshausenstr. 40, 24098 Kiel, Germany

<sup>2</sup> Institute Laue-Langevin, 6 rue Jules Horowitz, BP 156-38042 Grenoble, Cedex 9, France

<sup>3</sup> Institute of Physical Chemistry, RWTH Aachen University, Templergraben 59, 52056 Aachen, Germany; Fax +49 241 80 92327; richtering@rwth-aachen.de

(Received: March 18, 2004; published: July 9, 2004)

**Abstract:** The influence of shear flow on the structure of concentrated aqueous poly(*N*-isopropylacrylamide) solutions near the lower critical solution temperature was investigated by means of small-angle neutron scattering. Two samples, both in the semi-dilute regime above the overlap concentration, were studied. The scattering curve of the less concentrated sample was not influenced by shear flow, although high shear rates were reached. The more concentrated 4 wt.-% sample, however, displayed shear-induced demixing under strong shear flow conditions. Experiments at different shear stresses indicated the existence of a threshold shear stress and the phase separation process became faster with increasing stress. The two-dimensional scattering patterns remained isotropic even during the phase separation process and the correlation length as obtained from an Ornstein-Zernike plot increased. The influence of shear flow on the phase separation process is thus similar to a temperature increase. The results are in excellent agreement with data from recent rheo-optical experiments where shear-induced phase separation was also observed for the concentrated solution at high shear rates. Apparently, strong shear flow exerts an effect analogous to a temperature increase.

### Introduction

It is well known that shear flow can influence the phase separation of polymer solutions [1]. Several techniques have been employed to study the influence of shear on demixing of solutions of linear-chain polystyrene (PS) in dioctyl phthalate (DOP) including turbidity, dichroism, small-angle light scattering (SALS) and small-angle neutron scattering (SANS) [2-4]. With PS in DOP a so-called butterfly pattern in SALS and SANS which indicates shear-induced concentration fluctuations is often observed in semi-dilute solutions above the overlap concentration  $c^*$ . Butterfly scattering patterns have also been observed with polymer networks and some colloidal systems [5-9]. In these complex fluids the viscoelastic properties, especially the first normal stress difference, play an important role for the coupling between

density fluctuations and shear stress [10]. In further experiments with dilute PS/DOP solutions, shear-induced aggregation was observed below  $c^*$  indicating that entanglements may not be necessary for fluctuation enhancements [11].

Much less is known about aqueous polymer solutions where phase separation occurs upon heating. The temperature at which phase separation is first observed is known as the lower critical solution temperature (LCST). The most widely studied system displaying LCST behaviour in aqueous solution is poly(*N*-isopropylacrylamide) (PNiPAM) [12]. Temperature-sensitive PNiPAM polymers have been studied extensively, primarily due to their potential technological applications, including drug delivery systems and biotechnology [13,14]. PNiPAM undergoes a temperature-induced phase transition at the LCST of 31 - 34°C. The phase transition has varying effects depending on the architecture of the polymer system, whether linear-chain PNiPAM, chemically cross-linked microgels or macroscopic gels are discussed [12-14]. For dilute solutions of linear PNiPAM, the contraction of the polymer chain is observed with increasing temperature and the transition from an expanded coil to a compact globule occurs. Cross-linked microgels and macrogels exhibit a temperature-induced volume phase transition from a highly swollen to a collapsed state.

Only very recently, two groups reported on the influence of shear on the phase separation in aqueous PNiPAM solutions [15,16]. Badiger and Wolf observed shear-induced demixing in aqueous solutions of linear PNiPAM, which was attributed to the destruction of intersegmental clusters formed in the stagnant state. Wolf et al. suggested a general thermodynamic approach, in which the total energy of a polymer solution consists of the usual Flory-Huggins-Gibbs energy with an added term to describe the stored elastic energy [17]. Other approaches describe the dynamic coupling between concentration fluctuations and shear stress [18-20]. In this approach a stress applied causes squeezing of the solvent out of the more entangled regions, which consequently enhances the concentration fluctuations. In addition, aggregation, flocculation and for example the formation of large-scale bundle ordering have been observed in colloidal systems under shear [21].

Differences in the microstructures of colloidal and polymer solutions give rise to very different properties near the miscibility gap. Recently, we reported on the shear-induced phase separation of aqueous solutions of linear-chain PNiPAM and of suspensions of PNiPAM microgels. A shear-induced shift of the cloud curve to lower temperatures was observed in rheo-optical experiments for both polymer architectures [16].

Whereas optical techniques as, e.g., turbidity, probe concentration fluctuations on a rather large length scale, small-angle neutron scattering (SANS) is an important technique to investigate spatial heterogeneities on a length scale of few nanometers. The phase separation of concentrated PNiPAM solutions and gels in the quiescent state has been investigated by means of SANS by Shibayama et al. [22]. The scattering curves were fitted with an Ornstein-Zernike model and they observed that the correlation length diverged at the spinodal temperature.

In this contribution we investigate the influence of shear flow on the phase separation of concentrated aqueous solutions of linear-chain PNiPAM by means of small-angle neutron scattering. Analogue experiments with PNiPAM microgel solutions will be reported elsewhere [23].

## Experimental part

The linear-chain PNiPAM polymer was prepared based on the procedure described by Meewes et al. [16,24,25]. After recrystallization from a benzene-hexane solution the monomer *N*-isopropylacrylamide (NiPAM, 100.0 g, Aldrich) was dissolved in 2000 ml of pure water at 25°C. An aqueous solution of hydrogen peroxide (H<sub>2</sub>O<sub>2</sub>, 1 ml, 30 wt.-%, Merck) was added and the reaction mixture was degassed. The radical polymerization was started by opening the shutter of the UV lamp (Osram mercury vapour lamp Hg-10) and stopped after 35 min by closing the shutter and aerating the solution. The reaction mixture was poured into cold methanol (Aldrich) and was heated up slowly to 25°C. A fine precipitate of PNiPAM was decanted. For further purification the polymer was dissolved in methanol and cold water was added. The precipitate was decanted and another purification cycle was performed. Finally, the polymer was dissolved in water and isolated by freeze-drying.

In order to determine molecular weight  $M_w$ , radius of gyration  $R_g$  and second virial coefficient  $A_2$ , static light scattering experiments (SLS) in dilute solution were performed. From the extrapolation of  $Kc/R(q)$  to zero angle and zero concentration in the Zimm plots,  $R_g$  and  $A_2$  were determined. The weight-average molar mass  $M_w = 3.9 \cdot 10^6$  g/mol was obtained. The overlap concentration given by  $c^* = 3M_w/(4\pi R_g^3 N_L)$  was calculated. The temperature dependence of  $A_2$ ,  $R_g$  and  $c^*$  were given in detail previously [16]. At 25.8°C, which is below the LCST,  $R_g = 114$  nm,  $A_2 = 1.2 \cdot 10^{-4}$  mol·cm<sup>3</sup>/g<sup>2</sup> and  $c^* = 0.1$  wt.-% were obtained and at 36.5°C, which is above the LCST,  $R_g = 65$  nm,  $A_2 = -1.0 \cdot 10^{-6}$  mol·cm<sup>3</sup>/g<sup>2</sup> and  $c^* = 0.6$  wt.-% were found.

Small-angle neutron scattering experiments under shear (rheo-SANS) were performed at the instrument D11 of the Institute Laue-Langevin (ILL) in Grenoble, France. The neutron wavelength was  $\lambda = 6$  Å with a spread of  $\Delta\lambda / \lambda = 9\%$ . The data were collected on a two-dimensional multidetector (64 x 64 elements of 1 x 1 cm<sup>2</sup>), and corrected for background and empty cell scattering. Sample-detector distances of 36.0 and 10.5 m were employed. The incoherent scattering of H<sub>2</sub>O was used for absolute calibration according to standard procedures and software available at the ILL (GRAS<sub>ans</sub>P V. 3.25). A Bohlin CVO-120-HR rheometer was adjusted to the D11 beamline. Measurements were performed using a Searle shear cell of quartz cylinders with a gap of 1 mm. All experiments were carried out under isothermal conditions and the samples were allowed to equilibrate for 15 min at each temperature. The evolution of the temperature during the shear experiment was monitored employing a calibrated Pt-100 temperature sensor, which was placed directly to the outer wall of the glass shear cell. The sample temperature remained constant even during application of high shear stresses within an accuracy of  $\Delta T = \pm 0.2$  K. The scattering experiments were performed in the radial position yielding information in the plane formed by the flow and vorticity directions. Further processing of the isotropic two-dimensional SANS pattern was done by radially averaging to obtain a one-dimensional data set. All experiments were carried out at full contrast using D<sub>2</sub>O as the solvent.

## Results and discussion

Macromolecules form a transient network of entangled chains in semi-dilute polymer solution, where the polymer concentration  $c$  is above the overlap concentration  $c^*$ . The average distance between entanglement points is described by the so-called mesh size or correlation length  $\xi$ , which is large, compared to the size of a monomer

unit. For distances small compared to  $\xi$ , the polymer chain will exhibit single coil behaviour and possess a random or self-avoiding walk conformation. At larger distances, the semi-dilute solution emulates a polymer melt, since the sample space is densely packed with polymer segments of the blob size  $\xi$ . Consequently, for good solvent conditions  $I(q)$  should show a different behaviour than dilute solutions on length scales for  $\xi > 1/q$ . Here  $q = (4\pi/\lambda) \sin(\theta/2)$  denotes the magnitude of the scattering vector (with the scattering angle  $\theta$ ). The scattering intensity  $I(q)$  in the semi-dilute regime for  $\xi < 1/q$  is well described by the so-called Ornstein-Zernike equation, which is a Lorentzian function, and is given by

$$I(q) = \frac{I(0)}{1 + \xi^2 q^2} \quad (1)$$

where  $I(0)$  denotes the scattering intensity at  $q = 0$ . Fig. 1 shows the scattering intensity distribution normalized by concentration,  $I(q)/c$ , of PNiPAM solutions at different concentrations at 25°C and the corresponding Ornstein-Zernike plots of the same data. The scattering curves nicely overlap at high scattering vectors ( $q > 0.005 \text{ \AA}^{-1}$ ) and a slope of  $I(q) \propto q^{-1.65}$  is observed in the double logarithmic plot for all concentrations. Thus, the asymptotic scaling behaviour in the high  $q$ -regime is in good agreement with the predictions of the asymptotic  $q$ -dependence for a polymer in good solvent conditions according to the self-avoiding walk model, which predicts  $I(q) \propto q^{-1.66}$ . An increase of the scattering intensity in the low  $q$ -regime ( $q < 0.01 \text{ \AA}^{-1}$ ) is observed for the samples with concentrations of 0.50 and 4.60 wt.-%. At concentrations above the overlap concentration ( $c^* = 0.1 \text{ wt.-%}$  determined by SLS, see experimental details) additional long-range inhomogeneities are often observed giving rise to an increase of the scattering intensity. Correlation lengths  $\xi$  of  $1.8 \pm 0.1$  and  $1.3 \pm 0.1 \text{ nm}$  were obtained from Ornstein-Zernike fits for the 0.50 and 4.60 wt.-% samples, respectively, which agrees nicely with the data reported by Shibayama et al. [22]. The Ornstein-Zernike fits were performed in the high  $q$ -regime ( $q^2 = 0.005 - 0.035 \text{ \AA}^{-2}$ ). Thus the excess scattering in the low  $q$ -regime ( $q^2 < 0.005 \text{ \AA}^{-2}$ ), which is caused by the long-range inhomogeneities, is not taken into account.

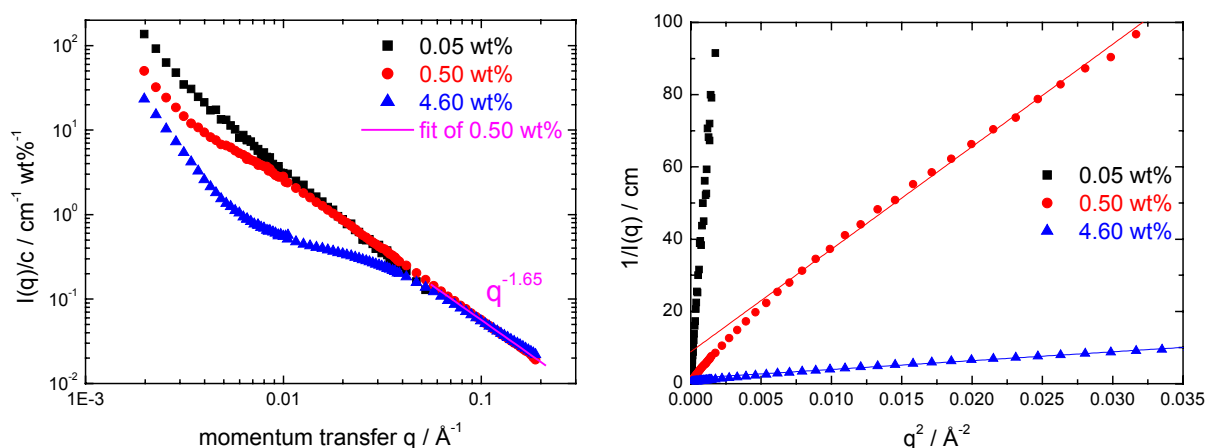


**Fig. 1.** Left: Scattering intensity distributions normalized by concentration,  $I(q)/c$ , of PNiPAM solutions at 25°C and different concentrations. Right: Ornstein-Zernike plot of the same SANS data

Fig. 2 displays results from a 1.1 wt.-% solution under different flow conditions at a constant temperature of 32.3°C, which is approximately 1K below the LCST in the

quiescent state. The top left part illustrates the shear protocol: the sample was sheared at different applied shear stresses and the evolution of shear rate and viscosity was recorded. At the lowest shear stress, the sample did not reach stationary shear flow, but at higher stresses the steady state was reached quickly. Shear thinning was found which is typical of concentrated polymer solutions and indicates that the shear rates were already above the characteristic relaxation time of the sample.

The other two plots in Fig. 2 display SANS data: first the angular-dependent scattering intensity is shown in a double logarithmic plot vs.  $q$  (top right). The bottom part shows an Ornstein-Zernike plot of the same data. The scattering intensity is well described by the Ornstein-Zernike equation (1) and it is apparent that shear flow has only little influence on the scattering intensity at this temperature. An average correlation length of  $\xi = 10.4 \pm 0.8$  nm was obtained. At this concentration the previously discussed rheo-turbidity measurements revealed no influence of shear flow on the phase separation as well [16].

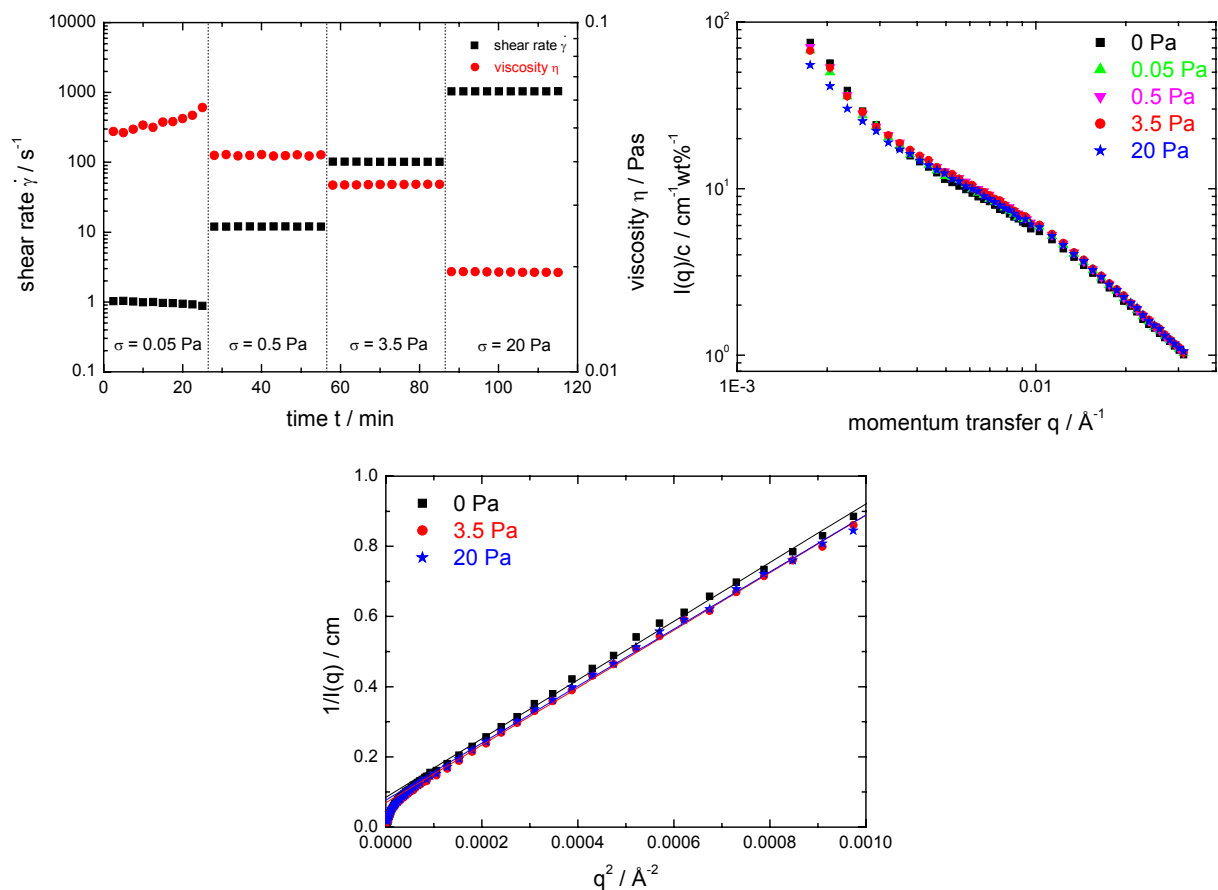


**Fig. 2.** Rheological and rheo-SANS data from a PNIPAM solution at 1.1 wt.-% and 32.3°C. The experiment was performed under controlled stress conditions. Top left: viscosity and shear rate; top right: SANS data; bottom: Ornstein-Zernike plot of SANS data

However, the scattering intensity was dramatically influenced by shear flow for the 4.0 wt.-% solution, see Fig. 3. The SANS intensity was strongly enhanced when a shear stress of 180 Pa was applied to the sample. The 2D scattering patterns remained isotropic at all shear stresses. Again the scattering intensity could be fitted

with the Ornstein-Zernike model except for the last data sets. The results are summarized in Tab. 1. Both, correlation length  $\xi$  and the forward scattering intensity  $I(q \rightarrow 0)$  strongly increased after application of high stress (180 Pa). Obviously, phase separation was induced by shear flow. It should be noted that the sample temperature ( $T = 32.3^\circ\text{C}$ ) was c. 1 K below the LCST and remained unchanged during the shear experiment within an accuracy of  $\Delta T = \pm 0.2$  K. These results agree nicely with rheo-optical data where shear-induced demixing was observed when the sample was subjected to strong shear flow. The scattering patterns we observed at high shear stress resemble those obtained by Shibayama et al. when the phase separation was induced by rising temperature [22].

As already mentioned above, the two-dimensional scattering patterns remained isotropic even at the highest applied stress. This indicates that the shear-induced demixing process is isotropic on a short, local length scale. Similar behaviour was observed with concentrated suspensions of PNIPAM microgels. Shear-induced demixing was also found and the scattering intensity at high  $q$  where the particle form factor is probed remained isotropic as well [23].

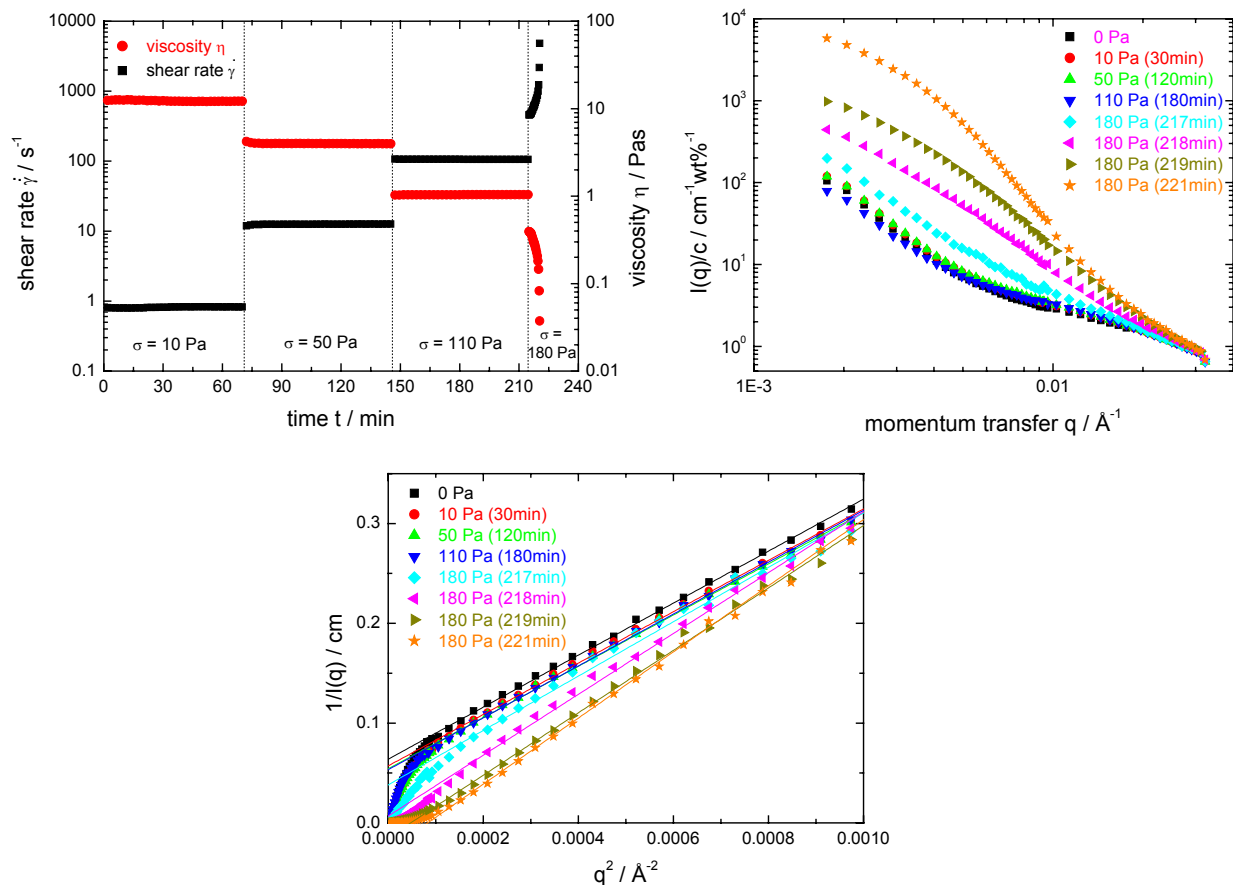


**Fig. 3.** Rheological and rheo-SANS data from a PNIPAM solution at 4.0 wt.-% and  $32.3^\circ\text{C}$ . The experiment was performed under controlled stress conditions. Top left: viscosity and shear rate; top right: SANS data; bottom: Ornstein-Zernike plot of SANS data

Results from a shear stress-up / shear stress-down experiment are shown in Fig. 4. The sample was presheared at 80 Pa where phase separation is not yet induced. Then the shear stress was increased to 165 Pa and the evolution of viscosity and

SANS intensity was recorded. Finally the shear stress was reduced back to 80 Pa. Apparently a shear stress of 165 Pa is also sufficient in order to induce phase separation. The phase separation process itself is fully reversible, when the stress is reduced to 80 Pa, the scattering curve relaxed back to its initial intensity. However, the shear-induced demixing process is slower at a shear stress of 165 Pa as compared to the experiment at 180 Pa. The kinetics of the demixing process for both shear stresses is compared in Fig. 5.

**Tab. 1.** Results from the Ornstein-Zernike fitting procedure of a PNiPAM solution at 4.0 wt.-% and 32.3°C (see Fig. 3). The errors were estimated to 10%

Time according to shear protocol in min	Shear stress and application time	$I(q \rightarrow 0) / \text{cm}^{-1}$	$\xi / \text{nm}$
0	0 Pa	$15.7 \pm 1.6$	$6.4 \pm 0.6$
30	10 Pa for 70 min	$17.5 \pm 1.8$	$6.7 \pm 0.7$
120	50 Pa for 75 min	$18.4 \pm 1.8$	$6.9 \pm 0.7$
180	110 Pa for 70 min	$18.7 \pm 1.9$	$7.0 \pm 0.7$
217	180 Pa for 2 min	$26.2 \pm 2.6$	$8.4 \pm 0.8$
218	180 Pa for 3 min	$145.8 \pm 14.6$	$21.1 \pm 2.1$

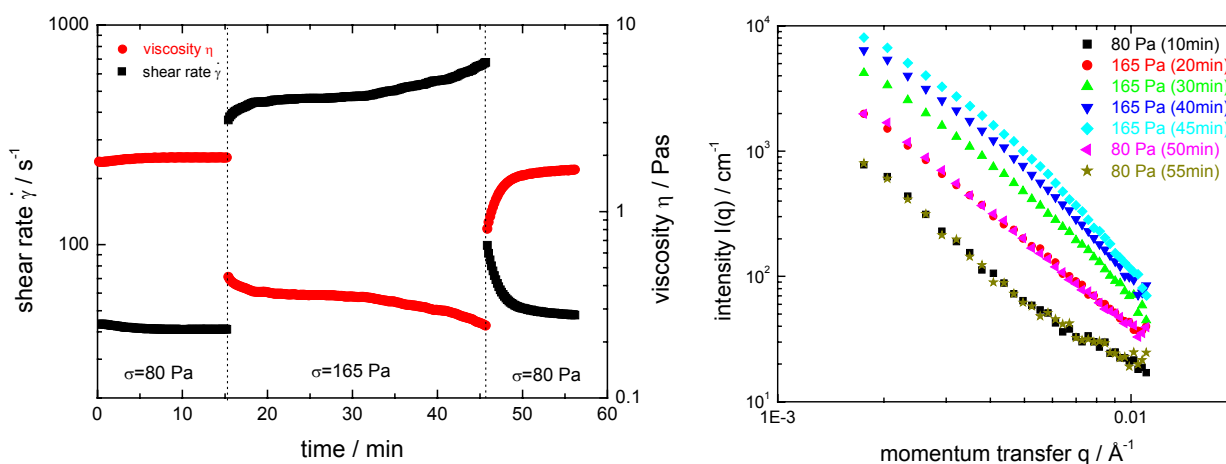


**Fig. 4.** PNiPAM solution at 4.0 wt.-% at 32.3°C under shear. Similar to Fig. 3, but at different shear stresses

At a shear stress of 165 Pa, the relative scattering intensities  $I(t)/I(t=0)$  obtained at  $q = 0.0021 \text{ \AA}^{-1}$  increased by a factor of c. 10 in c. 30 min. In contrast, application of a shear stress of 180 Pa for only 5 min gave rise to an increase of the low  $q$ -intensity by a factor of approximately 80. These experiments at different shear stresses indicate the existence of a threshold shear stress and the phase separation process becomes faster with increasing stress.

Phase separation in aqueous PNiPAM solutions is considered to be caused by hydrophobic interaction and the breaking of H-bonds and spectroscopic data showed a change of the polymer backbone conformation. Recently, Badiger and Wolf investigated a 2 wt.-% solution of PNiPAM ( $M_w = 1.6 \cdot 10^6 \text{ g/mol}$ ) in H<sub>2</sub>O and observed

shear-induced demixing in rheo-turbidity experiments. When the sample was heated at low shear rates they observed a viscosity increase just before the demixing temperature was reached and concluded that a physical network is formed. They interpreted the shear-induced phase separation in terms of a disruption of such favourable clusters. Similar rheological behaviour was observed in our case, see Fig. 6.

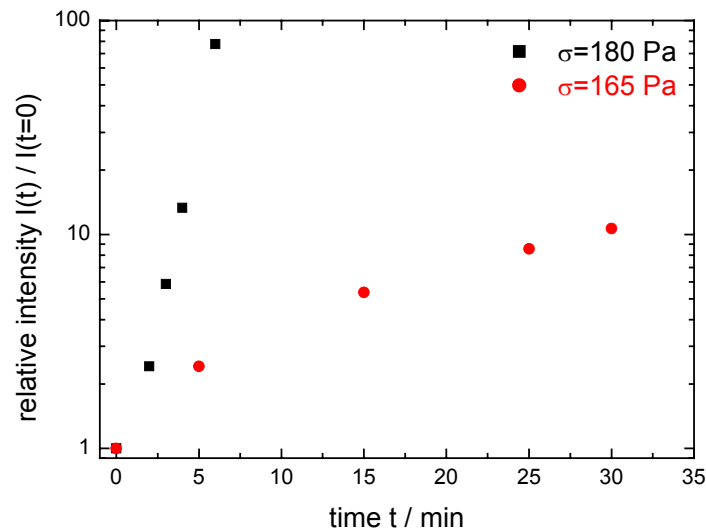


Fig. 5. Time-resolved relative SANS intensity  $I(t)/I(t=0)$  determined at  $q = 0.0021 \text{ \AA}^{-1}$  from a PNIPAM solution at 4.0 wt.-% at  $T = 32.3^\circ\text{C}$  (see Figs. 3 and 4). The application of the shear stresses (165 and 180 Pa) started at  $t = 0 \text{ min}$

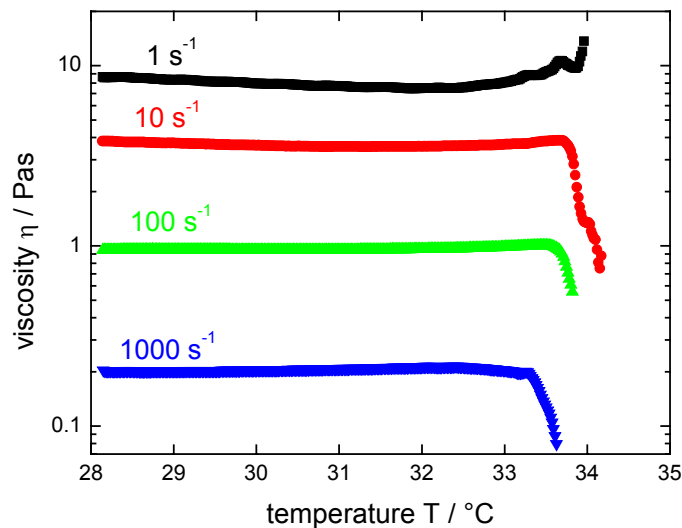


Fig. 6. Viscosity vs. temperature at different shear rates for a PNIPAM solution at 4.0 wt.-%

A formation of clusters has also been discussed in more complex polymer solutions as, e.g., in hydrophobically modified ethylhydroxyethylcellulose [26] or methylhydroxypropylcellulose [27]. In these cases an aggregation process via specific groups that are inhomogeneously distributed along the macromolecule is easily conceivable. In the present case of the PNIPAM homopolymer, all repeating units are chemically identical, which renders a cluster formation less imaginable. However, as

already mentioned above, specific interactions along the chain are considered to be responsible for the behaviour of PNiPAM in aqueous solution. Taking into account that semi-dilute polymer solutions reveal long-range heterogeneities (as, e.g., observed in scattering experiments, Fig. 1) a reversible network formation can be a good model to explain the viscosity increase near the demixing temperature as well as the observed shear enhanced phase separation. One could speculate that the strong shear flow induces a change of the polymer backbone conformation, which enhances phase separation. A stretching of the macromolecules should lead to an anisotropic structure which, however, was not found in the SANS experiments.

## Conclusions

The influence of shear flow on the structure of concentrated aqueous PNiPAM solutions is investigated by means of small-angle neutron scattering. The high  $q$  region of the scattering patterns at rest can be described by an Ornstein-Zernike approach and the correlation length decreases with concentration and increases with temperature in agreement with results by Shibayama et al.

The influence of shear flow on the solution structure close to the LCST is investigated for two samples, both at concentrations above the overlap concentration. The scattering curve of the less concentrated sample is not influenced by shear flow, although high shear rates are reached. The more concentrated 4 wt.-% sample, however, displays shear-induced demixing under strong shear flow conditions. Experiments at different shear stresses indicate the existence of a threshold shear stress and the phase separation process becomes faster with increasing stress.

The two-dimensional scattering patterns remain isotropic even during the phase separation process and the correlation length as obtained from an Ornstein-Zernike plot increases. The influence of shear flow on the phase separation process is thus similar to a temperature increase. The results are in excellent agreement with data from rheo-optical experiments where shear-induced phase separation was also observed for a concentrated solution at high shear rates. Apparently strong shear flow has an analogous effect as a temperature increase. Since the LCST of aqueous PNiPAM solutions is in an experimentally convenient temperature range, this system is ideal to investigate the kinetics of shear-induced phase separation. Such experiments are in progress and will be reported later.

Finally, we wish to note that shear-induced demixing is also observed with PNiPAM microgels, provided the cross-linking density is not too high. Rheo-SANS experiments showed that the particle collapse is isotropic, the aggregation however is anisotropic. Comparison of the properties of linear chains and internally cross-linked microgels indicates that a partial interpenetration of the macromolecules is necessary in order to induce phase separation by shear flow. The data suggest that both entanglements and specific interactions are responsible for the behaviour of aqueous PNiPAM solutions under shear.

**Acknowledgement:** Financial support by Deutsche Forschungsgemeinschaft is gratefully acknowledged. We thank Jaro Ricka and Rene Nyffenegger, University of Berne, Switzerland, for the possibility to prepare the linear-chain PNiPAM in their laboratory.

- [1] Rangel-Nafaile, C.; Metzner, A. B.; Wissbrun, K. F.; *Macromolecules* **1984**, *17*, 1187.
- [2] Morfin, I.; Lindner, P.; Boué, F.; *Macromolecules* **1999**, *32*, 7208.
- [3] Saito, S.; Hashimoto, T.; Morfin, J.; Lindner, P.; Boué, F.; *Macromolecules* **2002**, *35*, 445.
- [4] Saito, S.; Hashimoto, T.; *J. Chem. Phys.* **2001**, *114*, 10531.
- [5] Bastide, J.; Leibler, L.; Prost, J.; *Macromolecules* **1990**, *23*, 1821.
- [6] Moses, E.; Kume, T.; Hashimoto, T.; *Phys. Rev. Lett.* **1994**, *72*, 2037.
- [7] DeGroot, J. V.; Macosko, C. W.; Kume, T.; Hashimoto, T.; *J. Colloid Interface Sci.* **1994**, *166*, 404.
- [8] Belzung, B.; Lequeux, F.; Vermant, J.; Mewis, J.; *J. Colloid Interface Sci.* **2000**, *224*, 179.
- [9] Weigel, R.; Läuger, J.; Richtering, W.; Lindner, P.; *J. Phys. II France* **1996**, *6*, 529.
- [10] van Egmond, J. W.; *Macromolecules* **1997**, *30*, 8045.
- [11] Pönitsch, M.; Hollfelder, T.; Springer, J.; *Polym. Bull.* **1998**, *40*, 345.
- [12] Schild, H. G.; *Prog. Polym. Sci.* **1992**, *17*, 163.
- [13] Pelton, R.; *Adv. Colloid Interface Sci.* **2000**, *85*, 1.
- [14] Saunders, B. R.; Vincent, B.; *Adv. Colloid Interface Sci.* **1999**, *80*, 1.
- [15] Badiger, M.; Wolf, B. A.; *Macromol. Chem. Phys.* **2003**, *204*, 600.
- [16] Stieger, M.; Richtering, W.; *Macromolecules* **2003**, *36*, 8811.
- [17] Wolf, B. A.; *Macromolecules* **1984**, *17*, 615.
- [18] Helfand, E.; Fredrickson, G. H.; *Phys. Rev. E* **1989**, *62*, 2468.
- [19] Milner, S. T.; *Phys. Rev. E* **1993**, *48*, 3674.
- [20] Onuki, A.; *J. Phys. Condens. Matter* **1997**, *9*, 6119.
- [21] Vermant, J.; Raynaud, L.; Mewis, J.; Ernst, B.; Fuller, G. G.; *J. Colloid Interface Sci.* **1999**, *211*, 221.
- [22] Shibayama, M.; Tanaka, T.; Han, C. C.; *J. Chem. Phys.* **1992**, *97*, 6829.
- [23] Stieger, M.; Lindner, P.; Richtering, W.; *J. Phys. Condens. Matter*, submitted.
- [24] Meewes, M.; Ricka, J.; de Silva, M.; Nyffenegger, R.; Binkert, Th.; *Macromolecules* **1991**, *24*, 5811.
- [25] Kulicke, W.; Klein, J.; *Angew. Makromol. Chem.* **1987**, *96*, 169.
- [26] Badiger, M. V.; Lutz, A.; Wolf, B. A.; *Polymer* **2000**, *41*, 1377.
- [27] Schmidt, J.; Burchard, W.; Richtering, W.; *Biomacromolecules* **2003**, *4*, 453.